

Limit to the erbium ions emission in silicon-rich oxide films by erbium ion clustering

Nikola Prtljaga,^{1,*} Daniel Navarro-Urrios,² Andrea Tengattini,¹ Aleksei Anopchenko,¹ Joan Manel Ramírez,³ José Manuel Rebledo,^{3,4} Sònia Estradé,^{3,5} Jean-Philippe Colonna,⁶ Jean-Marc Fedeli,⁶ Blas Garrido,³ and Lorenzo Pavesi¹

¹*NanoScience Lab, Department of Physics, University of Trento, Via Sommarive 14, 38123 Povo, Trento, Italy*

²*Catalan Institute of Nanotechnology (CIN2-CSIC), Campus UAB, Edifici CM3, 08193 Bellaterra, Spain*

³*MIND-IN2UB, Departament D'Electrònica, Universitat de Barcelona, Carrer Martí i Franquès, 08 028 Barcelona, Spain*

⁴*Barcelona Materials Science Institute (ICMAB), CSIC, Campus UAB, Bellaterra 08193, Spain*

⁵*TEM-MAT, Scientific and Technological Centers, (CCIT), Universitat de Barcelona, Carrer Martí i Franquès, 08 028 Barcelona, Spain*

⁶*CEA/Leti, Minatec 17 rue des Martyrs, 38054 Grenoble cedex 9, France*

*nikolap@science.unitn.it

Abstract: We have fabricated a series of thin (~50 nm) erbium-doped (by ion implantation) silicon-rich oxide films in the configuration that mitigates previously proposed mechanisms for loss of light emission capability of erbium ions. By combining the methods of optical, structural and electrical analysis, we identify the erbium ion clustering as a driving mechanism to low optical performance of this material. Experimental findings in this work clearly evidence inadequacy of the commonly employed optimization procedure when optical amplification is considered. We reveal that the significantly lower erbium ion concentrations are to be used in order to fully exploit the potential of this approach and achieve net optical gain.

©2012 Optical Society of America

OCIS codes: (130.3130) Integrated optics materials; (160.5690) Rare-earth-doped materials; (250.5230) Photoluminescence; (310.6860) Thin films, optical properties.

References and links

1. D. Liang and J. E. Bowers, "Recent progress in lasers on silicon," *Nat. Photonics* **4**(8), 511–517 (2010).
2. A. Polman and F. C. J. M. van Veggel, "Broadband sensitizers for erbium-doped planar optical amplifiers: review," *J. Opt. Soc. Am. B* **21**(5), 871–895 (2004).
3. M. Fujii, M. Yoshida, Y. Kanzawa, S. Hayashi, and K. Yamamoto, "1.54 μm photoluminescence of Er³⁺ doped into SiO₂ films containing Si nanocrystals: evidence for energy transfer from Si nanocrystals to Er³⁺," *Appl. Phys. Lett.* **71**(9), 1198–1200 (1997).
4. G. Franzò, S. Boninelli, D. Pacifici, F. Priolo, F. Iacona, and C. Bongiorno, "Sensitizing properties of amorphous Si clusters on the 1.54-μm luminescence of Er in Si-rich SiO₂," *Appl. Phys. Lett.* **82**(22), 3871–3873 (2003).
5. I. Izeddin, D. Timmerman, T. Gregorkiewicz, A. Moskalenko, A. Prokofiev, I. Yassievich, and M. Fujii, "Energy transfer in Er-doped SiO₂ sensitized with Si nanocrystals," *Phys. Rev. B* **78**(3), 035327 (2008).
6. O. Jambois, F. Gourbilleau, A. J. Kenyon, J. Montserrat, R. Rizk, and B. Garrido, "Towards population inversion of electrically pumped Er ions sensitized by Si nanoclusters," *Opt. Express* **18**(3), 2230–2235 (2010).
7. I. Izeddin, A. S. Moskalenko, I. N. Yassievich, M. Fujii, and T. Gregorkiewicz, "Nanosecond dynamics of the near-infrared photoluminescence of Er-doped SiO₂ sensitized with Si nanocrystals," *Phys. Rev. Lett.* **97**(20), 207401 (2006).
8. C. J. Oton, W. H. Loh, and A. J. Kenyon, "Er³⁺ excited state absorption and the low fraction of nanocluster-excitable Er³⁺ in SiO_x," *Appl. Phys. Lett.* **89**(3), 031116 (2006).
9. B. Garrido, C. García, P. Pellegrino, D. Navarro-Urrios, N. Daldošo, L. Pavesi, F. Gourbilleau, and R. Rizk, "Distance dependent interaction as the limiting factor for Si nanocluster to Er energy transfer in silica," *Appl. Phys. Lett.* **89**(16), 163103 (2006).
10. O. Savchyn, F. Ruhge, P. Kik, R. Todi, K. Coffey, H. Nukala, and H. Heinrich, "Luminescence-center-mediated excitation as the dominant Er sensitization mechanism in Er-doped silicon-rich SiO₂ films," *Phys. Rev. B* **76**(19), 195419 (2007).
11. D. Navarro-Urrios, Y. Lebour, O. Jambois, B. Garrido, A. Pitanti, N. Daldošo, L. Pavesi, J. Cardin, K. Hijazi, L. Khomenkova, F. Gourbilleau, and R. Rizk, "Optically active Er³⁺ ions in SiO₂ codoped with Si nanoclusters," *J. Appl. Phys.* **106**(9), 093107 (2009).

12. D. Navarro-Urrios, F. Ferrarese Lapi, N. Prtljaga, A. Pitanti, O. Jambois, J. M. Ramírez, Y. Berencén, N. Daldozzo, B. Garrido, and L. Pavesi, "Copropagating pump and probe experiments on Si-nc in SiO_2 rib waveguides doped with Er: the optical role of non-emitting ions," *Appl. Phys. Lett.* **99**(23), 231114 (2011).
13. S. Cueff, C. Labbé, O. Jambois, B. Garrido, X. Portier, and R. Rizk, "Thickness-dependent optimization of Er^{3+} light emission from silicon-rich silicon oxide thin films," *Nanoscale Res. Lett.* **6**(1), 395 (2011).
14. C. A. Barrios and M. Lipson, "Electrically driven silicon resonant light emitting device based on slot-waveguide," *Opt. Express* **13**(25), 10092–10101 (2005).
15. J. T. Robinson, K. Preston, O. Painter, and M. Lipson, "First-principle derivation of gain in high-index-contrast waveguides," *Opt. Express* **16**(21), 16659–16669 (2008).
16. B. Garrido, C. García, S.-Y. Seo, P. Pellegrino, D. Navarro-Urrios, N. Daldozzo, L. Pavesi, F. Gourbilleau, and R. Rizk, "Excitable Er fraction and quenching phenomena in Er-doped SiO_2 layers containing Si nanoclusters," *Phys. Rev. B* **76**(24), 245308 (2007).
17. F. Iacona, C. Bongiorno, C. Spinella, S. Boninelli, and F. Priolo, "Formation and evolution of luminescent Si nanoclusters produced by thermal annealing of SiO_x films," *J. Appl. Phys.* **95**(7), 3723–3732 (2004).
18. F. Priolo, G. Franzò, D. Pacifici, V. Vinciguerra, F. Iacona, and A. Irrera, "Role of the energy transfer in the optical properties of undoped and Er-doped interacting Si nanocrystals," *J. Appl. Phys.* **89**(1), 264–272 (2001).
19. R. S. Quimby, W. J. Miniscalco, and B. Thompson, "Clustering in erbium-doped silica glass fibers analyzed using 980 nm excited-state absorption," *J. Appl. Phys.* **76**(8), 4472–4478 (1994).
20. P. Pellegrino, B. Garrido, J. Arbiol, C. García, Y. Lebour, and J. R. Morante, "Site of Er ions in silica layers codoped with Si nanoclusters and Er," *Appl. Phys. Lett.* **88**(12), 121915 (2006).
21. I. F. Crowe, R. J. Kashtiban, B. Sheriker, U. Bangert, M. P. Halsall, A. P. Knights, and R. M. Gwilliam, "Spatially correlated erbium and Si nanocrystals in coimplanted SiO_2 after a single high temperature anneal," *J. Appl. Phys.* **107**(4), 044316 (2010).
22. X. Wang, P. Li, M. Malac, R. Lockwood, and A. Meldrum, "The spatial distribution of silicon NCs and erbium ion clusters by simultaneous high-resolution energy filtered and Z-contrast STEM and transmission electron tomography," *Phys. Status Solidi., C Curr. Top. Solid State Phys.* **8**(3), 1038–1043 (2011).
23. D. A. Stanley, H. Alizadeh, A. Helmy, N. P. Kherani, L. Qian, and S. Zukotynski, "SEM-mapped micro-photonoluminescence studies of highly luminescent micro-clusters in erbium-doped silicon-rich silicon oxide," *J. Lumin.* **131**(1), 72–77 (2011).
24. M. Shah, M. Wojdak, A. J. Kenyon, M. P. Halsall, H. Li, and I. F. Crowe, "Rate equation modelling of erbium luminescence dynamics in erbium-doped silicon-rich-silicon-oxide," *J. Lumin.* (to be published).
25. A. Anopchenko, A. Tengattini, A. Marconi, N. Prtljaga, J. M. Ramírez, O. Jambois, Y. Berencén, D. Navarro-Urrios, B. Garrido, F. Milesi, J.-P. Colonna, J.-M. Fedeli, and L. Pavesi, "Bipolar pulsed excitation of erbium-doped nanosilicon light emitting diodes," *J. Appl. Phys.* **111**(6), 063102 (2012).
26. S. Minissale, T. Gregorkiewicz, M. Forcales, and R. G. Elliman, "On optical activity of Er^{3+} ions in Si-rich SiO_2 waveguides," *Appl. Phys. Lett.* **89**(17), 171908 (2006).
27. M. Wojdak, M. Klik, M. Forcales, O. Gusev, T. Gregorkiewicz, D. Pacifici, G. Franzò, F. Priolo, and F. Iacona, "Sensitization of Er luminescence by Si nanoclusters," *Phys. Rev. B* **69**(23), 233315 (2004).
28. G. Franzò, M. Miritello, S. Boninelli, R. Lo Savio, M. G. Grimaldi, F. Priolo, F. Iacona, G. Nicotra, C. Spinella, and S. Coffa, "Microstructural evolution of SiO_x films and its effect on the luminescence of Si nanoclusters," *J. Appl. Phys.* **104**(9), 094306 (2008).
29. C. Maurizio, F. Iacona, F. D'Acquisto, G. Franzò, and F. Priolo, "Er site in Er-implanted Si nanoclusters embedded in SiO_2 ," *Phys. Rev. B* **74**(20), 205428 (2006).
30. G. Franzò, E. Pecora, F. Priolo, and F. Iacona, "Role of the Si excess on the excitation of Er doped SiO_x ," *Appl. Phys. Lett.* **90**(18), 183102 (2007).
31. M. de Dood, L. Slooff, A. Polman, A. Moroz, and A. van Blaaderen, "Local optical density of states in SiO_2 spherical microcavities: theory and experiment," *Phys. Rev. A* **64**(3), 033807 (2001).
32. N. Daldozzo, D. Navarro-Urrios, M. Melchiorri, L. Pavesi, C. Sada, F. Gourbilleau, and R. Rizk, "Refractive index dependence of the absorption and emission cross sections at 1.54 μm of Er^{3+} coupled to Si nanoclusters," *Appl. Phys. Lett.* **88**(16), 161901 (2006).
33. N. Daldozzo, D. Navarro-Urrios, M. Melchiorri, L. Pavesi, F. Gourbilleau, M. Carrada, R. Rizk, C. García, P. Pellegrino, B. Garrido, and L. Cognolato, "Absorption cross section and signal enhancement in Er-doped Si nanocluster rib-loaded waveguides," *Appl. Phys. Lett.* **86**(26), 261103 (2005).
34. P. Horak, W. H. Loh, and A. J. Kenyon, "Modification of the Er^{3+} radiative lifetime from proximity to silicon nanoclusters in silicon-rich silicon oxide," *Opt. Express* **17**(2), 906–911 (2009).
35. L. Borowska, S. Fritzsche, P. G. Kik, and A. E. Masunov, "Near-field enhancement of infrared intensities for f-f transitions in Er^{3+} ions close to the surface of silicon nanoparticles," *J. Mol. Model.* **17**(3), 423–428 (2011).
36. E. M. Purcell, "Spontaneous emission probabilities at radio frequencies," *Phys. Rev.* **69**, 681 (1946).
37. E. Snoeks, A. Lagendijk, and A. Polman, "Measuring and modifying the spontaneous emission rate of erbium near an interface," *Phys. Rev. Lett.* **74**(13), 2459–2462 (1995).
38. H. Urbach and G. Rikken, "Spontaneous emission from a dielectric slab," *Phys. Rev. A* **57**(5), 3913–3930 (1998).
39. C. Creatore, L. C. Andreani, M. Miritello, R. Lo Savio, and F. Priolo, "Modification of erbium radiative lifetime in planar silicon slot waveguides," *Appl. Phys. Lett.* **94**(10), 103112 (2009).

1. Introduction

Erbium (Er^{3+})-doped silicon-rich oxide (SRO) films are studied as active material to a silicon-integrated optical amplifier or laser [1,2]. By using the sensitization action of silicon nanoclusters (Si-ncl) [3], limitations of the Er^{3+} excitation process are avoided (small absorption cross-section, spectrally narrow absorption lines [2]), and the overall material emission performance is improved [3–5]. At the same time, complementary-metal-oxide-semiconductor (CMOS) process compatibility is maintained, and emission in the third telecom window ($1.53 \mu\text{m}$) is achieved [1]. This allows for direct compatibility with the mainstream semiconductor technology, which yields mass manufacturing and heavy integration density of photonic devices [1]. Additional attractiveness is given by the possibility of electrical injection through electrical transport in the Si-ncl [6].

Despite these premises, optical gain achievement is still eluding. There is consensus in the literature that the principal reason obstructing the optical gain achievement in this material is a low fraction of sensitized erbium ions [7–10]. Recently, we have demonstrated that this is followed by the loss of light emission capability of Er^{3+} when embedded in SRO material [11]. While the main fraction of embedded erbium ions does not participate in the process of light emission, absorption properties of non-emitting ions remain unaltered [12]. Evidently, this becomes a major obstacle toward population inversion in this material. At this point, elucidating the origin of this phenomenon becomes of paramount significance for further material optimization and device development. In this work, we address this issue in a conclusive way and report on the mechanism responsible for it, i.e., erbium ion clustering.

2. Experiment

The samples used in this work are thin Er^{3+} -doped (by ion implantation) films of alternating SRO and SiO_2 layers deposited on a crystalline silicon wafer by low-pressure chemical vapor deposition (LPCVD) in a standard CMOS line. Thin films ($d \sim 50 \text{ nm}$) have the advantage that can be studied by electrical [6], optical [13] and optoelectronic means [14]. Deposition starts with a $d = 2 \text{ nm}$ thin SiO_2 layer deposited on p-type crystalline silicon wafer on top of which is deposited a $d = 3 \text{ nm}$ thick SRO layer with nominal silicon excess of 20 at. %. The procedure is repeated 10 times in order to reach the desired thickness of $d \sim 50 \text{ nm}$ for optimum performance in slot waveguide amplifier [15]. Finally, a $d = 2 \text{ nm}$ thin layer of SiO_2 is deposited on top. After deposition, samples are thermally treated in order to induce phase separation and amorphous silicon nanoparticles growth and formation ($T_{\text{annealing}} = 900^\circ\text{C}$ for $t = 1 \text{ h}$) [16,17]. Subsequently, the samples were implanted with erbium ions (dose: $1 \times 10^{15} \text{ at./cm}^2$ and energy: 20 keV) and thermally treated for a second time ($T_{\text{post-annealing}} = 800^\circ\text{C}$ for $t = 6 \text{ h}$) to recover implantation damage.

Photoluminescence (PL) measurements were done by employing the three different lines of an argon ion laser: $\lambda_{\text{exc}} = 488 \text{ nm}$ (resonant, excitation wavelength coincides with absorption line of Er^{3+}), $\lambda_{\text{exc}} = 476 \text{ nm}$ (non-resonant, Er^{3+} are excited by energy transfer from Si-ncl) and an additional line in UV $\lambda_{\text{exc}} = 361 \text{ nm}$ for the continuous wave (CW) visible PL measurements. In addition, a laser diode ($\lambda_{\text{exc}} = 974 \text{ nm}$, resonant) was used as well. Time-resolved (TR) PL measurements in the infrared were performed by modulating the laser beam with a mechanical chopper in the case of excitation with the argon ion laser, or by modulating the diode driving current by an external function generator in the case of excitation with the laser diode. For detection in the visible, a GaAs photomultiplier tube (PMT) for CW PL is used, and an InGaAs PMT is used for the IR (both CW and TR PL measurements). In the case of TR PL measurements in IR, the InGaAs PMT was interfaced with a multichannel scalar averager. In all cases before detection, the optical signal was spectrally filtered with a monochromator.

Electroluminescence (EL) spectra are collected using a fiber bundle and analyzed with a Spectra-Pro 2300i monochromator coupled with a nitrogen-cooled charge-coupled device (CCD) cameras (one in visible and one in IR). Emitted optical power and external quantum

efficiency (EQE) are measured using either a calibrated LED or a Ge photodiode. The acceptance angle of the photodiode is taken into account.

For transmission electron microscopy (TEM), a JEOL 2010-FEG (200kV) scanning transmission electron microscope was used, equipped with a GIF spectrometer for STEM-EELS and EFTEM imaging mode. Samples for TEM observations were prepared through conventional mechanical polishing with a final Ar⁺ bombardment using a PIPS Gatan system. Erbium concentrations were determined by secondary ion mass spectrometry (SIMS) calibrated with a sample of known erbium concentration. The silicon excess was calculated with the formula $(1 - x/2)/(1 + x)$, with $x = [O]/[Si]$ as measured by x-ray photon spectroscopy (XPS).

3. Results and discussion

The erbium concentration profile in our thin films has been determined by SIMS, and it is reported in Fig. 1(a). The peak concentration $n_{\text{peak}} = 5.2 \times 10^{20}$ at./cm³ is located in the center of the active layer, at approximately $d \sim 20$ nm below the sample surface. The average erbium concentration is $n_{\text{average}} = 2.9 \times 10^{20}$ at./cm³. A silicon excess of 9 at. % was determined by XPS. The thickness of the active material $d \sim 44$ nm was found by TEM (see Appendix A). Note that this Er³⁺ concentration was chosen based on previous reports that indicate long lifetimes and high emission intensities, i.e., no cooperative photoluminescence quenching effects [18].

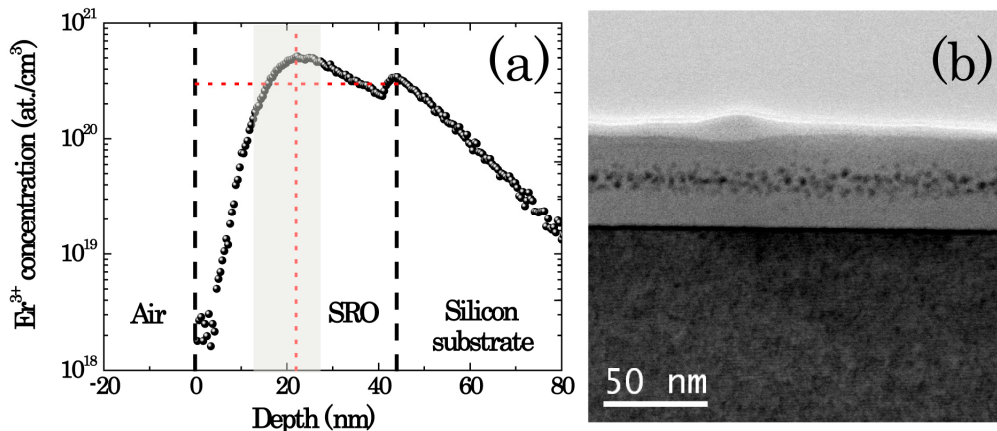


Fig. 1. (a) Semi-log plot of erbium concentration profile in the studied samples obtained by SIMS. Thick vertical dashed lines indicate interfaces between air/SRO and SRO/silicon substrate. Vertical red dotted line corresponds to the peak Er³⁺ concentration, and the horizontal red dotted line to an average Er³⁺ concentration in the active layer. The shaded area corresponds to the layer where erbium clusters are visible in TEM images. (b) Bright field scanning TEM (STEM) image of the sample.

Surprisingly, erbium clusters are visible as a dark spotted layer in TEM image (Fig. 1(b)). This erbium cluster layer is located at $d \sim 20$ nm below the sample surface, and it is approximately 15 nm wide (see Fig. 1(b)). It contains $55 \pm 5\%$ of the total number of erbium ions (shaded area in Fig. 1(a)). This is a first insight on what could limit the Er³⁺ emission capability as the clustered erbium ions emit light very inefficiently [19]. However, not all of the Er³⁺ in this layer may be clustered and, on the other hand, owing to the finite resolution of TEM, the erbium clustered region could be wider, as small erbium clusters (formed by a few atoms only) may escape detection. Thus, we correlate these findings with the results of a spectroscopic analysis.

It is worth mentioning that similar local inhomogeneity in erbium ions spatial distribution and the tendency to clusterize in silicon rich oxide films have been reported previously in thin films prepared with very different deposition techniques [20–24]. Thus, this type of behavior

is not inherent to LPCVD but is quite general for Er³⁺ concentrations larger than 10²⁰ at./cm³ [20–24].

Er³⁺ emission can be observed in our samples both by non-resonant (Fig. 2(a) - $\lambda_{\text{exc}} = 476$ nm with an excitation photon flux $\Phi_{\text{exc}} = 3 \times 10^{20}$ ph./cm²) and resonant optical excitation, as well as by electrical excitation (see Appendix B). In Fig. 2(b), a visible PL spectrum under CW UV optical excitation ($\lambda_{\text{exc}} = 364$ nm, $\Phi_{\text{exc}} = 3 \times 10^{18}$ ph./cm²) is also reported. The broad PL band in Fig. 2(b) situated at $\lambda = 750$ nm is attributed to residual Si-ncl PL. The additional peak at 550 nm, which is observable only under UV optical excitation or electrical bias, could be associated with direct excited state emission ($^4S_{3/2} - ^4I_{15/2}$ radiative Er³⁺ transition) visible owing to its high emission cross section. Moreover, the presence of cooperative upconversion (CUC) processes are observed by the shortening of the lifetimes of the 1.535 μm Er³⁺ emission with increased excitation photon flux (Fig. 3(a) - $\lambda_{\text{exc}} = 476$ nm, excitation photon flux varies from $\Phi_{\text{exc}} = 2.8 \times 10^{18}$ ph./cm² to 2.7×10^{20} ph./cm²).

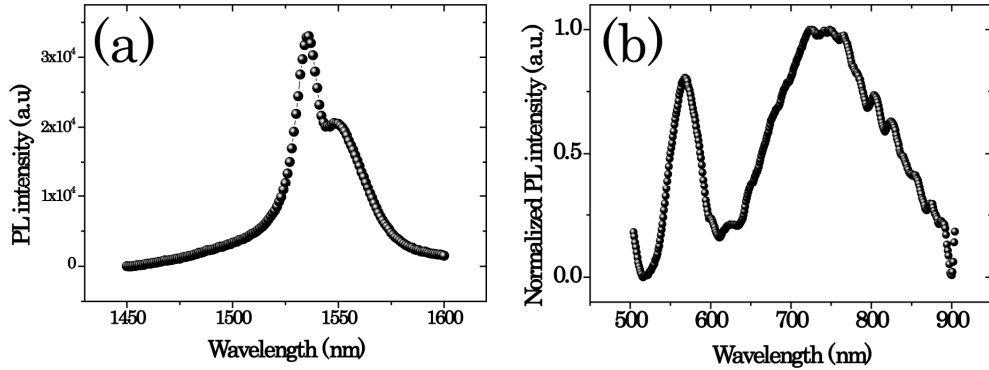


Fig. 2. (a) PL spectrum of the $^4I_{13/2} - ^4I_{15/2}$ radiative erbium transition in the studied sample under non-resonant optical excitation. (b) Normalized visible PL spectrum under CW UV optical excitation.

In order to evaluate the fraction of Er³⁺ that emits light efficiently, n_{active} , CUC has been quantified with the method of [16]. The PL measurements were carried out by resonant ($\lambda_{\text{exc}} = 974$ nm) and non-resonant ($\lambda_{\text{exc}} = 476$ nm) optical excitation. The experimental data were fitted by Eq. (1) [16]:

$$\frac{1}{\tau_{PL}(\Phi_{\text{exc}})} = \frac{n_2 * C_{up}}{\ln(1 + \tau_0 * n_2 * C_{up})} \quad (1)$$

where n_2 is the excited state population of erbium ions at $t_0 = 0$, and C_{up} is the CUC's coefficient; τ_0 is the Er³⁺ decay time in the absence of CUC, τ_{PL} is the measured Er³⁺ emission decay time and Φ_{exc} is the excitation photon flux. In both cases (resonant and non-resonant optical excitation), the same results (within experimental error) were found.

An example of the fit of experimental data by Eq. (1) is reported in Fig. 3(a) ($\lambda_{\text{exc}} = 476$ nm). The fit yields $C_{up} = 2.1 \pm 0.3 \times 10^{-15}$ cm³/s, and $\tau_0 = 2.13 \pm 0.05$ ms. This is a long lifetime considering the estimated radiative lifetimes in these samples (7 ms, see Appendix C). It is worth noticing that this same material shows a very high EQE under electrical bias (~0.4%) [25].

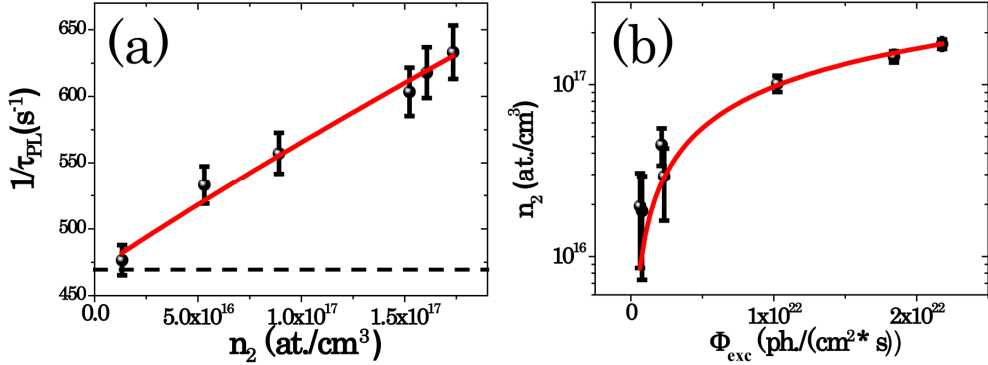


Fig. 3. (a) The best fit (red line) of experimental data (black spheres) obtained using non-resonant optical excitation by Eq. (1). Dashed horizontal line represents the time decay in absence of cooperative upconversion. (b) The best fit (red line) of experimental data (black squares) obtained using resonant optical excitation by Eq. (2).

C_{up} is significantly higher than the previously reported value for similar Er^{3+} concentrations [9], although it is in agreement with the large erbium clustering observed in TEM images. Note that C_{up} represents an average value, and the local C_{up} can vary significantly across the active layer owing to the Er^{3+} concentration profile (see Fig. 1(a)).

Knowing C_{up} and σ_{abs} , the direct Er^{3+} absorption cross-section (measured value agrees with those reported in [11] within the experimental errors), n_{active} can be estimated by fitting the experimental data obtained using resonant optical excitation ($\lambda_{exc} = 974 \text{ nm}$) with the following Eq. (2) (Fig. 3(b)) [11]:

$$n_2 = \frac{\left[(\sigma_{abs}(974\text{nm}) * \Phi_{exc} + \frac{1}{\tau_0})^2 + 4 * \sigma_{abs}(974\text{nm}) * C_{up} * n_{active} * \Phi_{exc} \right]^{1/2}}{2 * C_{up}}$$

$$- \frac{(\sigma_{abs}(974\text{nm}) * \Phi_{exc} + \frac{1}{\tau_0})}{2 * C_{up}}. \quad (2)$$

It is found $n_{active} = 2.1 \pm 0.2 \times 10^{18} \text{ at./cm}^3$. This accounts for approximately $0.72 \pm 0.11\%$ of the total Er^{3+} content measured by SIMS.

This number is significantly lower than the non-clustered fraction estimated from TEM (~45%). However, in the TEM images only clusters of certain size can be seen (few nm of size). Thus, if erbium clusters consist of only few erbium ions they will not be observed by TEM, although they will heavily influence the optical properties of the active material. This explains the observations of previous reports, even though higher fractions of active erbium ions were reported [11,26,27]. Therefore, Er^{3+} clustering is the main phenomenon that limits n_{active} .

While different fabrication protocols could lead to different matrix quality [28] and consequently, a different local Er^{3+} environment [29], loss of emission capability of erbium ions is a frequently reported issue [11,20,21], indicating a similar quenching mechanism. This is here studied on samples made by LPCVD. Furthermore, variations in silicon excess (0 at.% - 10 at.%) and thermal treatment do confirm the data presented here. We studied variation in annealing temperatures (900°C – 1100°C), duration (5 – 60 min.) and methods (furnace or rapid thermal processing)

Although we observe a certain variations in n_{active} and CUC's coefficient among different samples, the degree of these variations (n_{active} being always $\leq 1\%$ of total Er^{3+} content) is not

sufficient to provide an amplifier material (which requires $n_{\text{active}} > 50\%$) or to change the overall picture. For sake of completeness, we have not found appreciable difference in SIMS profiles and TEM images between different samples.

It is important to emphasize that in these samples, a significant fraction of erbium ions is situated in the silica layers that prevent the suggested silicon excess induced Er^{3+} ion de-excitation [30]. Moreover, n_{active} is determined by using a sub-bandgap (for Si-ncl) resonant (for Er^{3+}) optical excitation, avoiding the possibility of energy back-transfer toward the Si-ncl [7]. Furthermore, we would like to stress the fact that no optical gain was reported in this material (silicon-rich oxide) with high Er^{3+} concentration ($> 1 \times 10^{20} \text{ at./cm}^3$) regardless of the particular deposition technique used. Thus, we conclude that the erbium ion clustering is the main mechanism responsible for the low optical activity of Er^{3+} ions in this material at the used erbium concentration ($\sim 10^{20} \text{ at./cm}^3$).

Therefore, to achieve full Er^{3+} inversion (i.e. net optical gain), the Er^{3+} concentration should be decreased significantly with respect to the usually considered optimum value of $n_{\text{Er}^{3+}} \sim 10^{20} \text{ at./cm}^3$ [18]. This will reduce the maximum gain value achievable.

4. Conclusions

In summary, thin erbium-doped films of alternating layers of SRO and silica were fabricated and characterized in a configuration that mitigates previously proposed mechanisms for loss of light emission capability of erbium ions [7,8,30]. Even though promising results in terms of erbium PL lifetime (~2 ms) and EQE under electrical bias have been obtained, the main fraction of erbium ions does not contribute efficiently to the light emission owing to erbium ion clustering. The only possibility left to achieve net gain in this material system is to decrease the Er^{3+} concentration to level where clustering no longer occurs.

Appendix A: Structural analysis of the samples

Energy filtered (EFTEM) TEM image of the sample obtained by filtering at 15 eV (c-Si plasmon peak) is reported in Fig. 4(a). An active layer, approximately 44 nm thin, can be clearly seen, with the SRO (bright lines) and oxide layer (darker lines) visible. Erbium clusters can be seen close to the center of the active layer (dark spots in Fig. 4(a)) their chemical nature confirmed by HAADF (Fig. 4(b)) - bright line in the center of the layer corresponds to a high concentration of erbium ($Z = 68$) clusters, EFTEM and EELS (not shown). These clusters lay at $d \approx 20 \text{ nm}$ and extend in a region 15 nm thick.

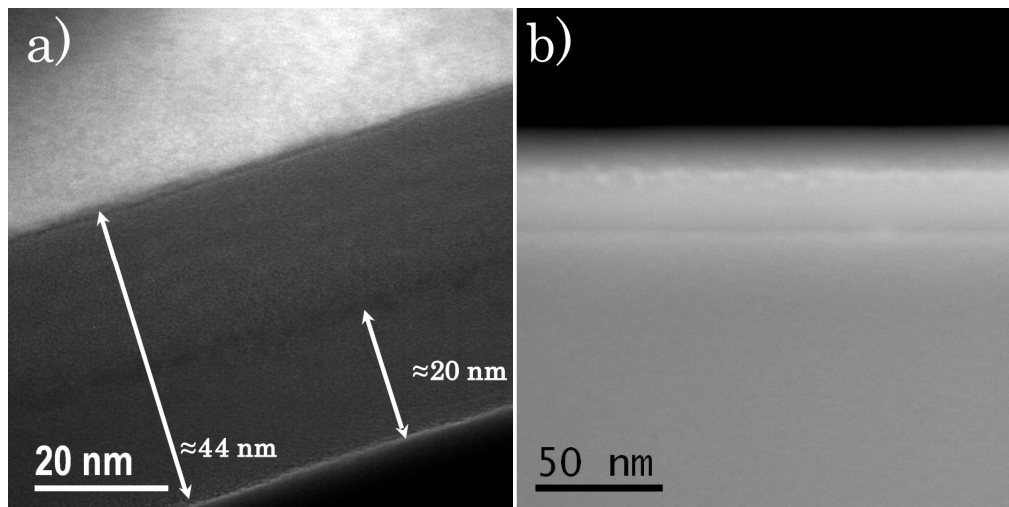


Fig. 4. (a) EFTEM image of the sample. (b) High angle annular dark field STEM image of the sample.

Appendix B: Electroluminescence (EL) spectrum of the samples

EL spectrum of the samples in the IR obtained with an injected current of $I = 100 \mu\text{A}$ and a forward bias of $U = 45.1 \text{ V}$ is reported in Fig. 5. This spectrum, owing to the $^4\text{I}_{13/2} - ^4\text{I}_{15/2}$ erbium radiative transition, resembles the one obtained under optical excitation (Fig. 2(a)).

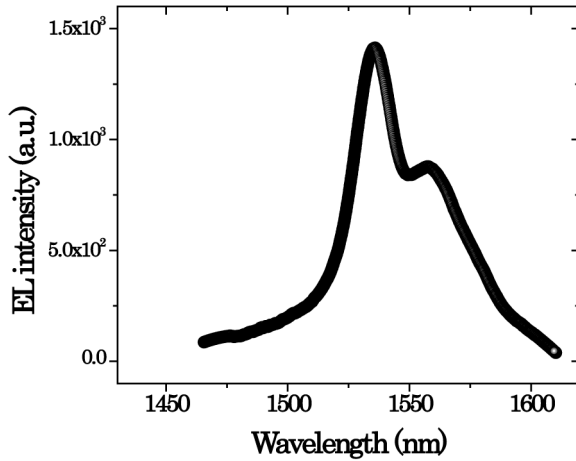


Fig. 5. EL spectrum of the $^4\text{I}_{13/2} - ^4\text{I}_{15/2}$ radiative erbium transition in the studied samples.

Appendix C: Erbium radiative lifetime estimate

To estimate the CUC's coefficient [16] and the fraction of Er^{3+} , which can emit efficiently [11], we estimate the Er^{3+} radiative lifetime. In the literature, it is reported that Er^{3+} in a bulk silica has a radiative lifetime $\tau_{\text{rad}} = 18 \text{ ms}$ [31]. However, since in SRO films refractive index is different than in SiO_2 [32], the radiative lifetime of Er^{3+} changes. Considering the silicon excess (9 at.%) and literature reports [6,16,27,32,33], a radiative lifetime of $\tau_{\text{rad}} \sim 10 \text{ ms}$ can be estimated in our films.

This value is also what is expected for bulk samples when accounting for the near-field enhancement of radiative rate in vicinity of silicon nanoparticles ($\tau_{\text{rad}} = 10 \text{ ms}$ [34] - $\tau_{\text{rad}} = 7 \text{ ms}$ [35]). Finally, since we are using thin films deposited on a high refractive index material (silicon substrate), a certain enhancement of the radiative rate is expected [36–39], and therefore we assumed a value of $\tau_{\text{rad}} = 7 \text{ ms}$.

Acknowledgments

This work was supported by EC through the project ICT-FP7-224312 HELIOS and by Italy-Spain integrated actions. D. N.-U. thanks the financial support of AGAUR through the Beatriu de Pino's program and J.-M. R. thanks the CSIC for a JAE predoc grant. Authors would like to acknowledge the Laboratory of Electron NanoScopy, MIND-IN2UB, Dept. Electrònica, and the Scientific and Technological Centers (Universitat de Barcelona). A. Ruiz-Caridad, F. Peiró, Y. Berencén and O. Jambois are acknowledged for electron microscopy analysis and fruitful discussion. We acknowledge the contributions from N. Daldosso and A. Marconi at an early stage of the work.